8

Application of Recurrent Radon Precursors for Forecasting Local Large and Moderate Earthquakes

Ming-Ching T. Kuo
National Cheng Kung University
Taiwan

1. Introduction

Measurement of radon-222 in groundwater has been frequently used in earthquake prediction (Igarashi et al. 1995; Liu et al. 1985; Noguchi & Wakita 1977; Teng, 1980; Wakita et al. 1980; Kuo et al. 2006, 2010a, 2010b). According to a worldwide survey (Hauksson 1981; Toutain & Baubron 1999), more than 80 % of radon (Rn-222) anomalies associated with earthquakes show increases in radon concentration precursor to a rupture while a few anomalies manifested decreases in radon. The purpose of this chapter is to provide a practical guide of monitoring groundwater radon for the early warning of local disastrous earthquakes. In this chapter, methods of monitoring groundwater radon including procedures of sample collection and radon determination will be addressed. The following sections outline suitable geological conditions to consistently catch precursory declines in groundwater radon, in-situ radon volatilization mechanism for interpreting anomalous decreases in groundwater radon prior to earthquakes, and mathematical model for quantifying gas saturation developed in newly created cracks preceding an earthquake. Case studies are provided to illustrate the application of recurrent radon precursors for forecasting local large and moderate earthquakes.

2. Sample collection radon determination

Accurate sampling for radon measurements depends on appropriate monitoring wells. Because radon concentration in groundwater relates to emanation rates of geological layers, representative sampling must be from properly constructed wells. A submersible pump is commonly used in monitoring wells for groundwater sampling except artesian wells. Every sampling starts with flushing the stagnant water in the well and especially in the screen zone. Inadequate purging can be a major source of error, because the water sample is a mixture of stagnant water from the well bore, pore water from the filter gravel and groundwater influenced by the natural emanation rate of the aquifer. Fig. 1 shows the radon concentration in the well discharge during continuous sampling in a monitoring well. During the first period of flushing, the radon concentration of the water samples is practically zero and then increases rapidly to 529 pCi/L. The mean radon concentration measured for this monitoring well was 529 ± 19 pCi/L (eleven samples). A minimum of 3 well-bore volumes was purged before taking samples for radon measurements.

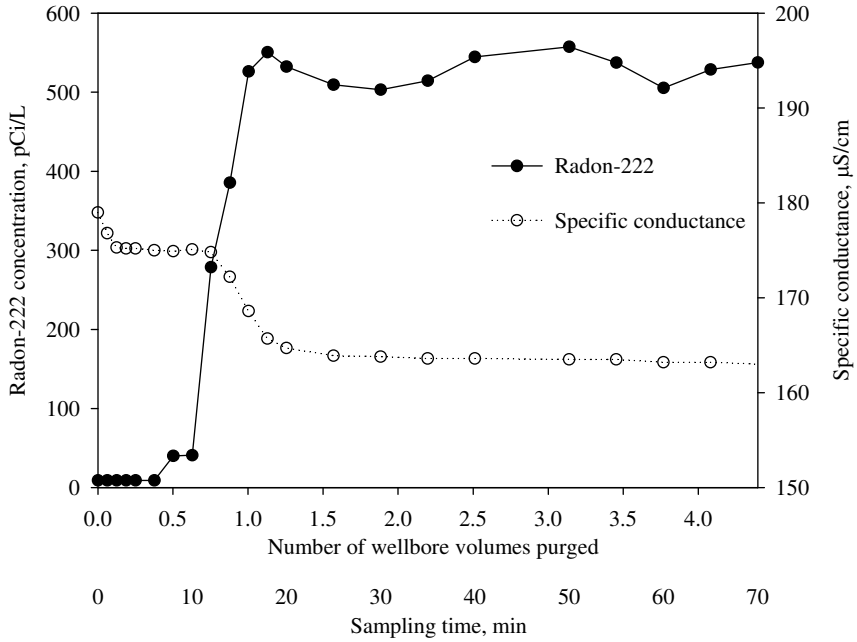

Fig. 1. Radon concentration and electrical conductivity in the well discharge during continuous sampling in a deep observation well

A 40-ml glass vial with a TEFLON lined cap was used for sample collection. After collecting a sample, the sample vial was inverted to check for air bubbles. If any bubbles were present, the sample was discarded and the sampling procedure repeated. The date and time of sampling was recorded and the sample stored in a cooler. The maximum holding time before analysis was 4 days.

For the determination of the activity concentration of radon-222 in groundwater, a modified method described by Prichard and Gesell (1977) was adopted. Radon was partitioned selectively into a mineral-oil scintillation cocktail immiscible with the water sample (Noguchi 1964). The sample was dark-adapted and equilibrated, and then counted in a liquid scintillation counter (LSC) using a region or window of the energy spectrum optimal for radon alpha particles (Lowry 1991).

Radon concentrations were determined by drawing a 15-ml sample directly from a field sample into a clean syringe. Care was taken to prevent aeration of the samples in the process. The samples were then injected beneath a 5-ml layer of mineral-oil-based scintillation solution in 24-ml vials. The vials were vigorously shaken to promote phase contact, dark-adapted and held for at least three hours to ensure equilibrium between radon-222 and its daughters, and then assayed with a liquid scintillation counter. The results were corrected for the amount of radon decay between sampling and assay.

The results of the measurements were determined in units of counts per minute (cpm). It was essential to ensure that only the activity of radon-222 was measured. Using the TRI-CARB software of Packard 1600TR, it was possible to view the alpha spectrum (Fig. 2). The peaks of radon-222 (5.49 MeV), polonium-218 (6.00 MeV) and polonium-214 (7.69 MeV) can be distinguished.

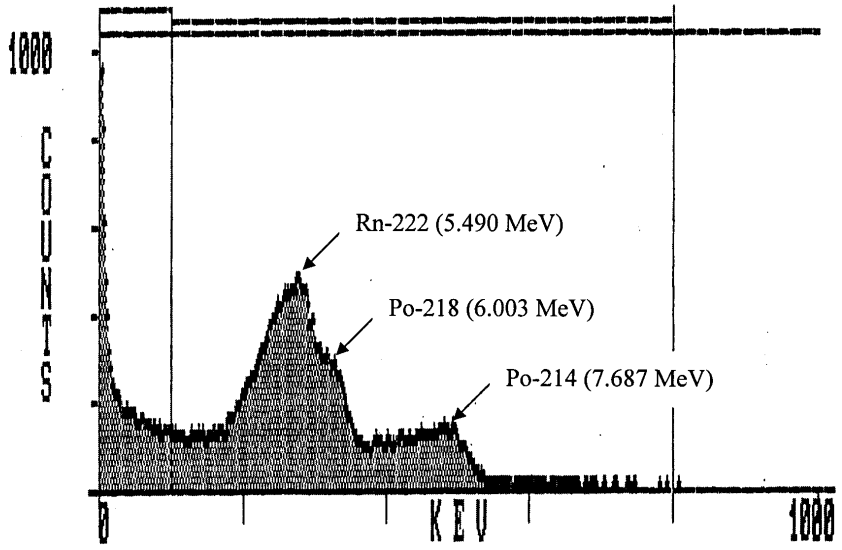

Fig. 2. Alpha spectrum of radon-222 and its daughter nuclides represented by TRI-CARB software

A calibration factor for the LSC measurements of 7.1 ± 0.1 cpm/pCi (Fig. 3) was calculated using an aqueous Ra-226 calibration solution, which is in secular equilibrium with Rn-222 progeny. For a count time of 50 min and background less than 6 cpm, a detection limit below 18 pCi/L was achieved using the sample volume of 15-ml (Prichard et al. 1992).

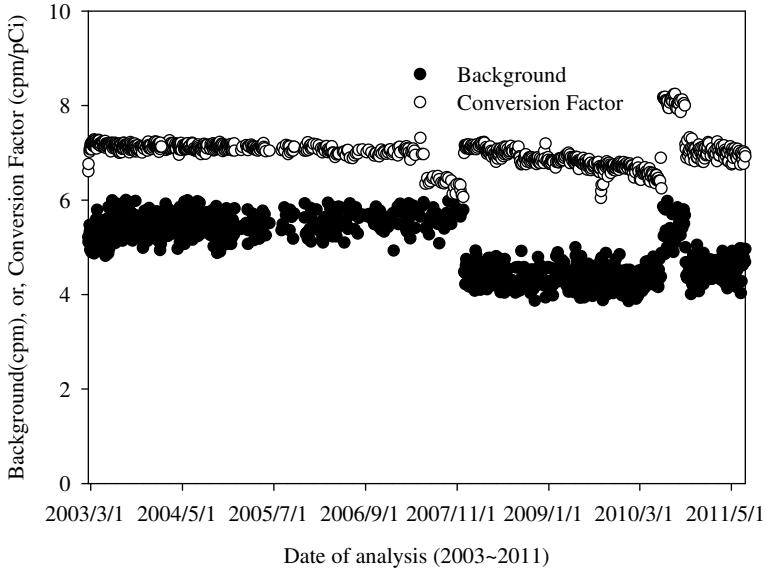

Fig. 3. Calibration factor and background for LSC measurements

Verification of radon-222 as the radioisotope responsible for activity in the well water tested was obtained by the repeated counting of three samples from two wells. The half-life of 3.841 days experimentally determined for samples from Well Liu-Ying (I) located in Tainan Plain, Taiwan compares favorably with the accepted value of 3.825 days as shown in Fig. 4. When the counting vials are lack of tightness, radon will escape from counting vials and the half-life times experimentally determined for samples will be apparently shorter. Fig. 4 also shows an example of such a case from Well Wen-Tsu (II) located in Choshui River Alluvial Fan, Taiwan.

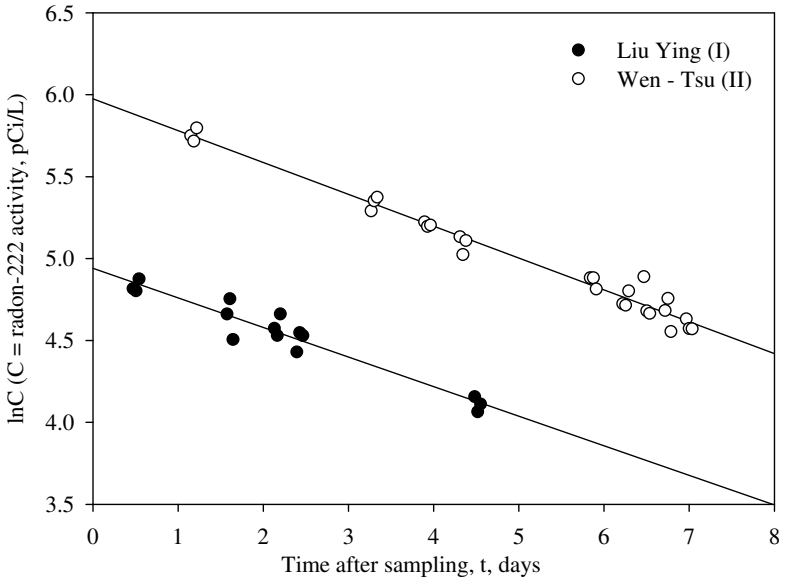

Fig. 4. Measurement of half life from semi-logarithmic decay curve

3. Suitable geological conditions to catch recurrent radon precursors

The 2003 Chengkung earthquake of magnitude (M) 6.8 on December 10, 2003 was the strongest earthquake near the Chengkung area in eastern Taiwan since 1951. The Antung radon-monitoring well (D1, Fig. 5) was located 20 km from the epicenter. Approximately 65 days prior to the 2003 Chengkung earthquake, precursory changes in radon concentration in ground water were observed. Specifically, radon decreased from a background level of 780 pCi/L to a minimum of 330 pCi/L (Fig. 6). Both geological conditions near the Antung hot spring and the vapor-liquid phase behavior of radon were investigated to explain the anomalous decrease of radon precursory to the 2003 Chengkung earthquake.

The production interval of the well ranges from 167 m to 187 m below ground surface and is pumped more or less continuously for water supply purposes. Discrete samples of geothermal water were collected for analysis of radon (Rn-222) twice per week. Liquid scintillation method was used to determine the activity concentration of radon-222 in ground water (Noguchi 1964; Prichard et al. 1992). The radon concentration was fairly stable (780 pCi/L in average) from July 2003 to September 2003 (Fig. 6). Sixty-five days before the magnitude (M) 6.8 earthquake (December 10, 2003), the radon concentration of ground

water started to decrease and continued to decrease for 45 days. Twenty days prior to the earthquake, the radon concentration reached a minimum value of 330 pCi/L and before starting to increase. Just before the earthquake, the radon concentration recovered to the previous background level of 780 pCi/L. The main shock also produced a sharp anomalous coseismic decrease (~300 pCi/L). After the earthquake, some irregular variations were observed, which we interpret as an indication that the strain release by the main shock was not complete and that some accumulation and release of strain continued in the region.

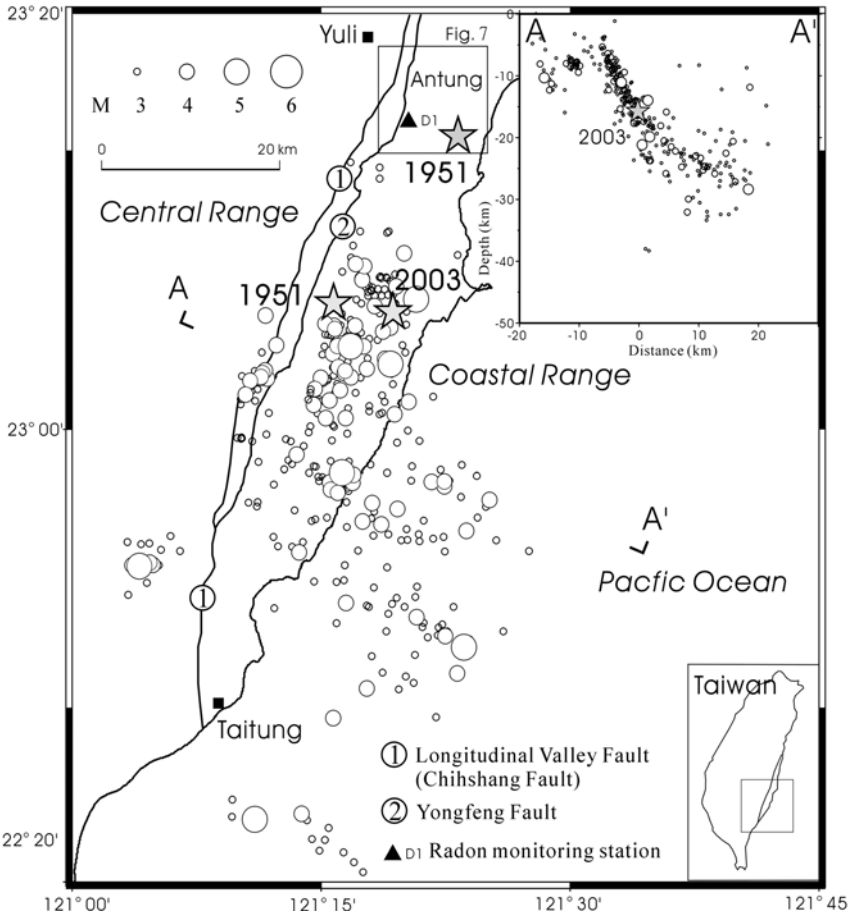

Fig. 5. Map of the epicentral and hypocentral distributions of the mainshock and aftershocks of the 2003 Chengkung earthquake and 1951 mainshocks (star: mainshock, open circles: aftershocks).

The Antung hot spring (Fig. 7) is in a unique tectonic setting located at the boundary between the Eurasian and Philippine Sea plates near the Coastal Range. Four stratigraphic units are present. The Tuluanshan Formation consists of volcanic units such as lava and volcanic breccia as well as tuffaceous sandstone. The Fanshuliao and Paliwan Formations

consist of rhythmic sandstone and mudstone turbidites. The Lichi mélange occurs as a highly deformed mudstone that is characterized by penetrative foliation visible in outcrop. The Antung hot spring is situated in a brittle tuffaceous-sandstone block surrounded by a ductile mudstone of the Paliwan Formation (Chen & Wang 1996). Well-developed minor faults and joints are common in the tuffaceous-sandstone block displaying intensively brittle deformation. It is possible that these fractures reflect deformation and disruption by the nearby faults. Hence, geological evidence suggests the tuffaceous-sandstone block displays intensively brittle deformation and develops in a ductile-deformed mudstone strata. Ground water flows through the fault zone and is then diffused into the block along the minor fractures.

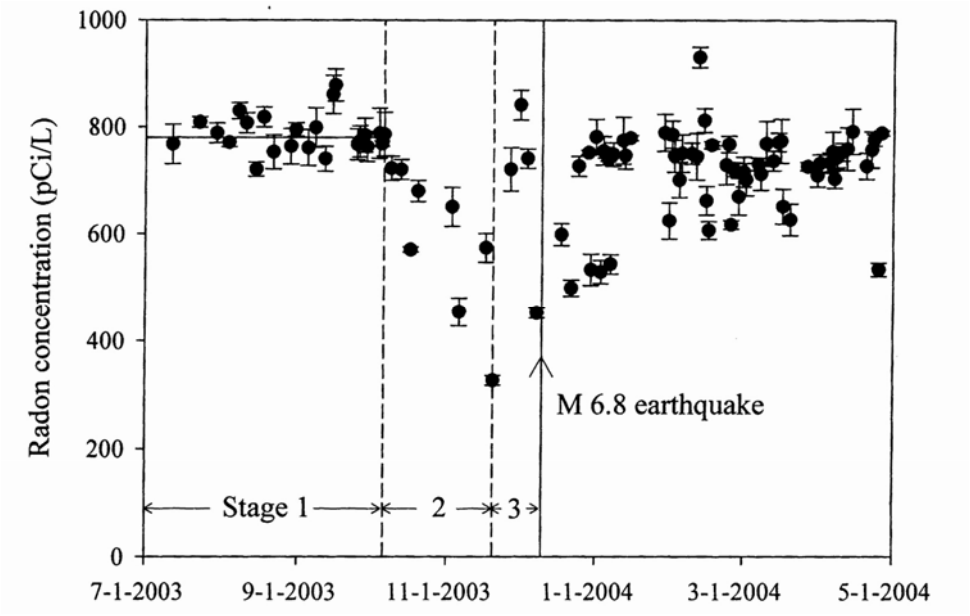

Fig. 6. Radon concentration data at the monitoring well (D1) in the Antung hot spring. Stage 1 is buildup of elastic strain. Stage 2 is dilatancy and development of cracks and gas saturation. Stage 3 is influx of ground water and diminishment of gas saturation.

Under geological conditions such as those of the Antung hot spring, we hypothesized that when regional stress increases, dilation of the rock mass occurs at a rate faster than the rate at which pore water can flow into the newly created pore volume (Brace et al. 1966; Scholz et al. 1973). During this stage (Stage 2 in Fig. 6), gas saturation and two phases (vapor and liquid) develop in the rock cracks. Meanwhile, the radon in ground water volatilizes and partitions into the gas phase and the concentration of radon in ground water decreases. Thus, the sequence of events for radon data prior to the 2003 Chengkung earthquake (Fig. 6) can be interpreted in three stages. From July 2003 to September 2003 (Stage 1), radon was fairly stable (around 780 pCi/L). During this time, there was an accumulation of tectonic strain, which produced a slow, steady increase of effective stress. Sixty-five days before the magnitude (M) 6.8 earthquake, the concentration of radon started to decrease and reached a

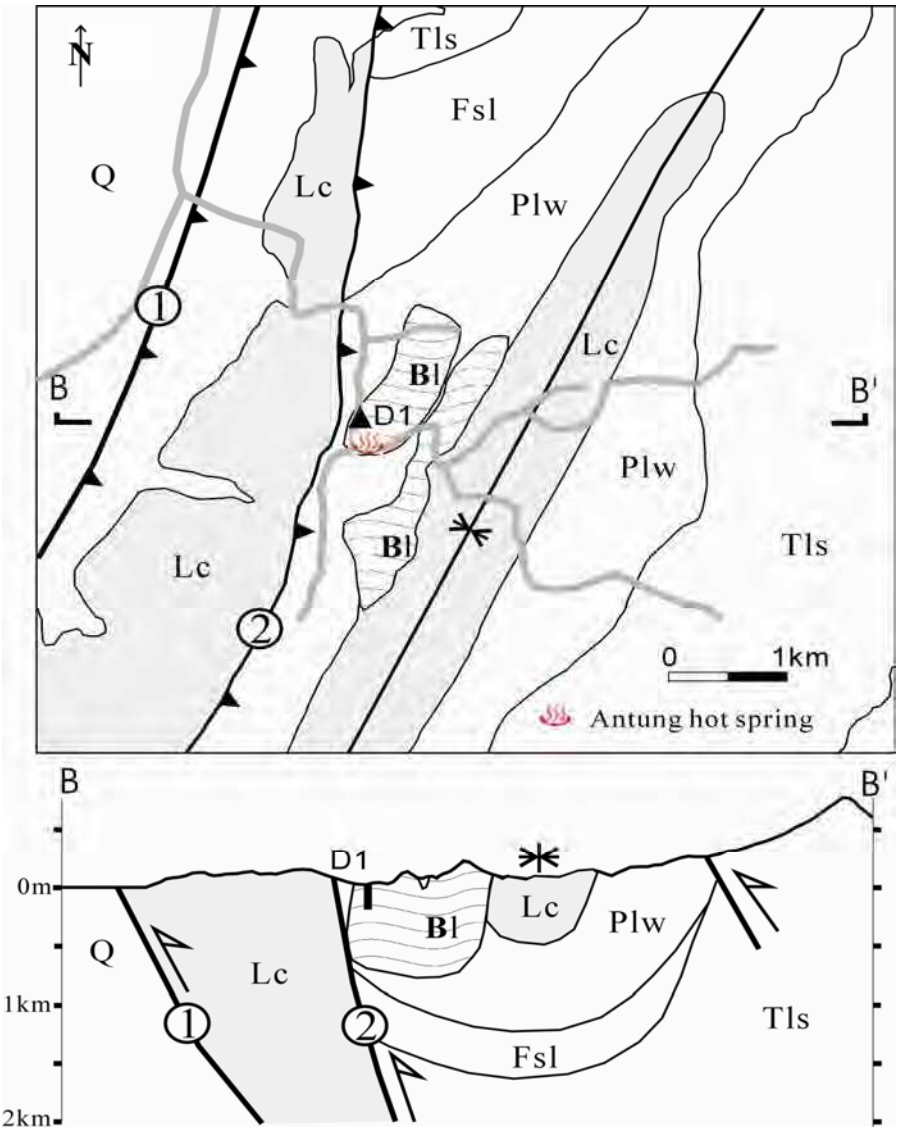

Fig. 7. Geological map and cross section near the radon-monitoring well in the area of Antung hot spring (Q: Holocene deposits, Lc: Lichi mélange, Plw: Paliwan Formation, Fsl: Fanshuliao Formation, Tls: Tuluanshan Formation, Bl: tuffaceous fault block, D1: radon-monitoring well, : Chihshang, or, Longitudinal Valley Fault, : Yongfeng Fault). See Fig. 6 for map location.

minimum value of 330 pCi/L twenty days before the earthquake. During this 45-day period (Stage 2), dilation of the rock mass occurred and gas saturation developed in cracks in the

rock and radon volatilized into the gas phase. Stage 3 started at the point of minimum radon concentration when water saturation in cracks and pores began to increase and radon increased and recovered to the background level. The main shock produced a sharp coseismic anomalous decrease (~300 pCi/L). After the earthquake, some irregular variations were observed, which we attribute to strain release as some accumulation and release of strain continued in the region.

4. In-situ radon volatilization mechanism

Radon partitioning into the gas phase can explain the anomalous decreases of radon precursory to the earthquakes (Kuo et al., 2006). To support the hypothesis of radon volatilization from ground water into the gas phase, radon-partitioning experiments were conducted to determine the variation of the radon concentration remaining in ground water with the gas saturation at formation temperature (60 ℃) using formation brine from the Antung hot spring. Five levels of gas saturation were investigated, specifically S_g = 5 %, 10 %, 15 %, 20 %, and 25 % where S_g is gas saturation. Triplicate experiments were conducted for each level of gas saturation. Every experiment started with 40-ml of formation brine. Five levels of headspace volume at 2 ml, 4 ml, 6 ml, 8 ml, and 10 ml were then created above the liquid phase for five levels of gas saturation at 5 %, 10 %, 15 %, 20 %, and 25 %, respectively. Two-phase equilibrium was achieved for each experiment in 30 minutes at the formation temperature (60 ℃).

A kinetic study of radon volatilization from ground water into the gas phase was conducted to determine the time required to reach equilibrium. In the kinetic experiment, formation brine from the Antung hot spring with an initial radon concentration of 479 ± 35 pCi/L was used. Every sample started with 40-ml formation brine and a headspace volume at 6 ml was then created above the liquid phase. A total of five samples were prepared. The radon concentration remaining in ground water was determined at various volatilization times (i.e., 2 min, 5 min, 15 min, 30 min, and 60 min). The time required to reach equilibrium for radon volatilization was only about 5 minutes.

Data from the vapor-liquid two-phase equilibrium radon-partitioning experiments (Fig. 8) were regressed with the two-phase partitioning model to determine Henry's coefficient as follows.

$$C_0 = C_w (H \times S_g + 1) \quad (1)$$

where C_0 is initial radon concentration in groundwater precursory to each radon anomaly, pCi/L; C_w is the radon minimum in groundwater observed in well D1 during an anomalous decline, pCi/L; S_g is gas saturation, fraction; H is Henry's coefficient for radon at formation temperature (60 ℃), dimensionless. Fig. 8 shows the regressed line with H = 12.8 and R^2 = 0.9919 (regression coefficient). Henry's coefficient for radon at 60 ℃ determined for the Antung formation brine (12.8) is higher than the value (7.91) for water at 60 ℃ (Clever, 1979). Fig. 8 can be used to estimate the amount of gas saturation required for various decreases in concentration of radon. For example, the anomalous decrease of radon concentration from 780 pCi/L to 330 pCi/L required a gas saturation of 10 % in cracks in the rock.

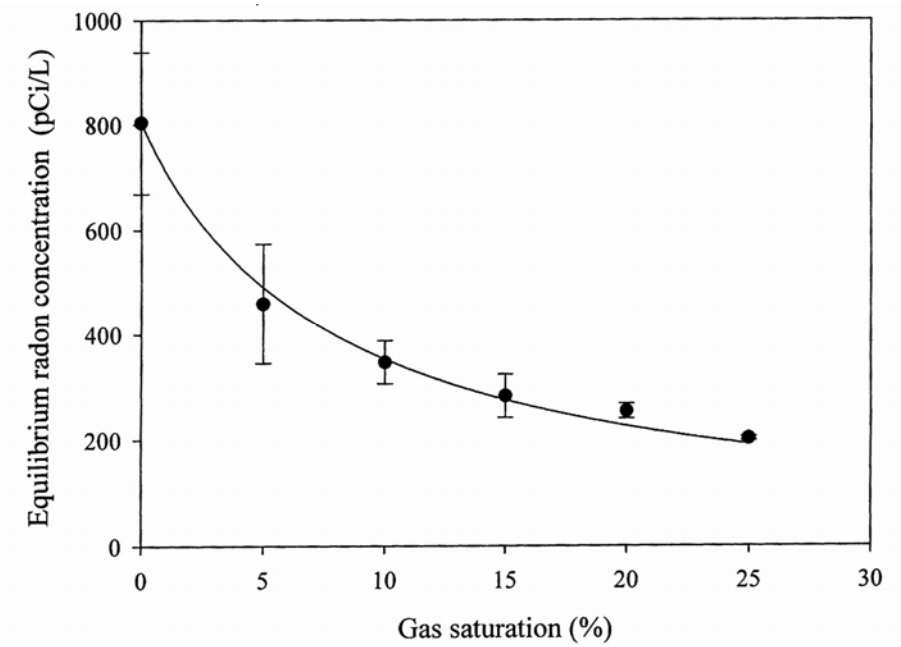

Fig. 8. Variation of radon concentration remaining in ground water with gas saturation at 60 °C using formation brine from the Antung hot spring.

5. Case study

We have monitored groundwater radon since July 2003 at well D1 at the Antung hot spring that is located about 3 km southeast of the Chihshang fault (Fig. 9). The Chihshang fault is part of the eastern boundary of the present-day plate suture between the Eurasia and the Philippine Sea plates. The Chihshang fault ruptured (Hsu, 1962) during two 1951 earthquakes of magnitudes M = 6.2 and M = 7.0. The annual survey of geodetic and GPS measurements has consistently revealed the active creep of the Chihshang fault that is moving at a rapid steady rate of about 2-3 cm/yr during the past 20 years (Angelier et al., 2000; Yu & Kuo, 2001; Lee et al., 2003).

Fig. 10 shows the radon concentration data since July 2003 at the monitoring well (D1) in the Antung hot spring. Radon-concentration errors are ±1 standard deviation after simple averaging of triplicates. Recurrent groundwater radon anomalies were observed to precede the earthquakes of magnitude M_w = 6.8, M_w = 6.1, M_w = 5.9, and M_w = 5.4 that occurred on December 10, 2003, April 1, 2006, April 15, 2006, and February 17, 2008 at the Antung D1 monitoring well. We consider the M_w 5.9 earthquake that occurred on April 15, 2006 triggered by stress transfer in response to the 2006 M_w 6.1 Taitung earthquake. All the three recurrent anomalous decreases observed at Antung follow the same v-shaped progression and are marked with green inverted triangles in Fig. 10. Environmental records such as atmospheric temperature, barometric pressure, and rainfall were examined to check whether the radon anomaly could be attributed to these environmental factors. The

atmospheric temperature, barometric pressure, and rainfall are periodic in season. It is difficult to explain such a large radon decrease by these environmental factors. There was also no heavy rainfall responsible for the radon anomaly.

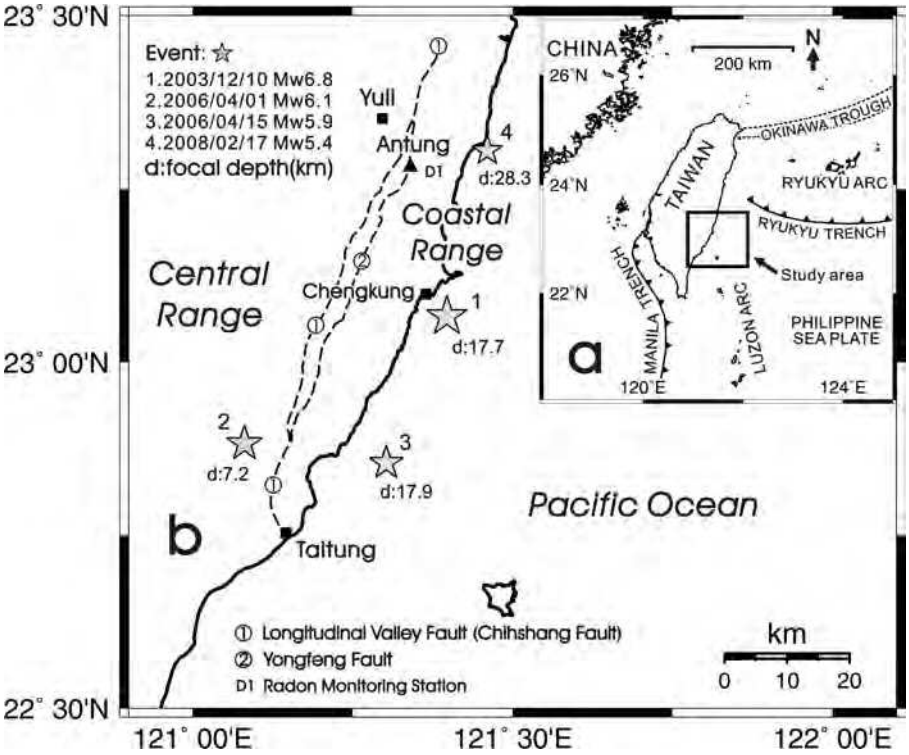

Fig. 9. Map of the epicenters of the earthquakes that occurred on December 10, 2003, April 1 and 15, 2006, February 17, 2008 near the Antung hot spring. (a) Geographical location of Taiwan. (b) Study area near the Antung hot spring.

The box-and-whisker plot is used on the right-hand side in Fig. 10. It shows the median (50th percentile, 764 pCi/L) as a center bar, and the quartiles (25th and 75th percentiles, 692 pCi/L and 849 pCi/L) as a box. The whiskers (456 pCi/L and 1077 pCi/L) cover all but the most extreme values in the data set. Based on the box-and-whisker plot, the threshold concentration of anomalous radon minima at the Antung D1 monitoring well is estimated as 456 pCi/L. The radon minimum recorded prior to the 2008 M_w = 5.4 Antung earthquake is close to the threshold concentration and can be easily masked by the noisy background. On

the other hand, the radon anomalous minima, recorded precursory to strong earthquakes ($M_w > 6.0$), the 2003 M_w = 6.8 Chengkung and 2006 M_w = 6.1 Taitung earthquakes, are low enough to be clearly distinguished from the background noise.

The radon minima, measured prior to local moderate earthquakes, are easily masked by the noisy background. Fig. 10 also shows the large background variation in radon data following the 2003 M_w = 6.8 Chengkung, 2006 M_w = 6.1 Taitung, and 2008 M_w = 5.4 Antung earthquakes. Four local earthquakes with magnitudes (M_w) of 5.5, 5.2, 6.2, and 5.2 occurred on 12/11/2003, 1/1/2004, 5/19/2004, and 9/26/2005, respectively. Based upon their magnitudes and locations, we consider these as aftershocks and induced events of the 2003 Chengkung earthquake. The large scatter in radon data between the 2003 M_w = 6.8 Chengkung and 2006 M_w = 6.1 Taitung earthquakes can be related to these aftershocks. The 2006 Mw 6.1 Taitung earthquake also triggered the Mw 5.9 earthquake that occurred on April 15, 2006. One local earthquake of magnitude M_w = 4.9 that occurred on 6/4/2006 can be considered as an aftershock of the 2006 M_w = 6.1 Taitung earthquake. The M_w = 4.9 aftershock also caused a large scatter in radon data following the 2006 M_w = 6.1 Taitung earthquake. The large background variation in radon data following the 2008 M_w = 5.4 Antung earthquake can also be attributed to local earthquakes, such as a local earthquake of magnitude M_w = 5.3 that occurred on 12/2/2008.

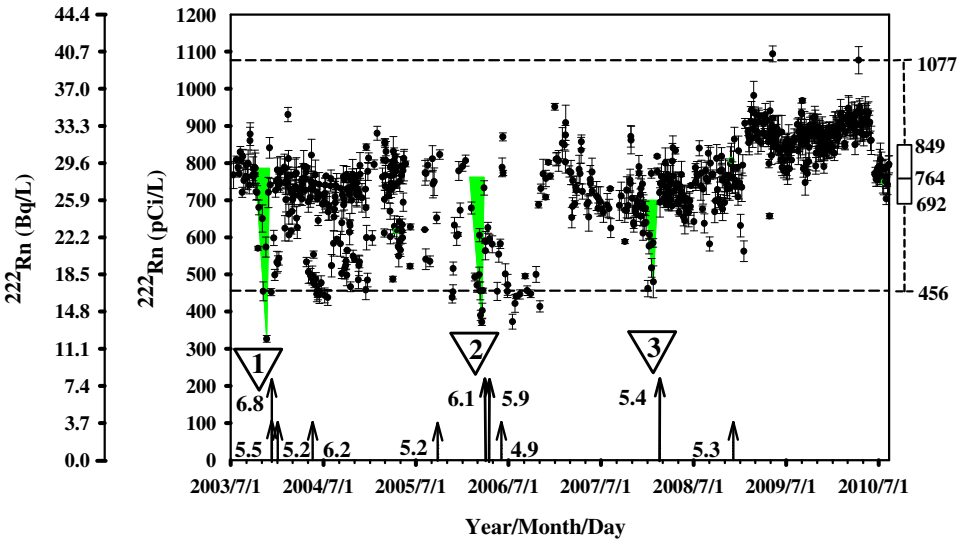

Fig. 10. Radon concentration data at well D1 in the Antung hot spring (open inverted triangles: anomalous radon minima; green inverted triangles: v-shaped pattern; long arrows: mainshocks; short arrows: aftershocks; earthquake magnitude M_w shown beside arrows).

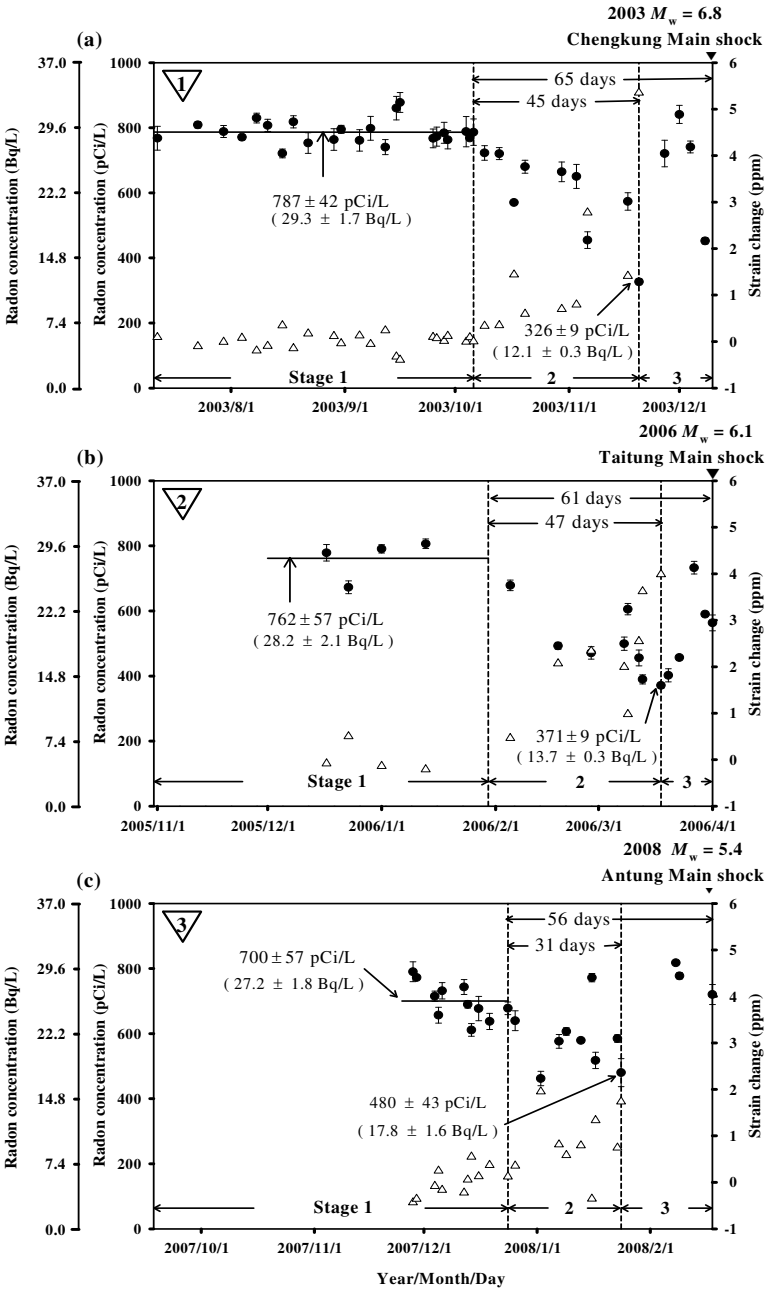

Fig. 11. Observed radon anomalies at well D1 prior to (a) 2003 Chengkung, (b) 2006 Taitung, and (c) 2008 Antung earthquakes. Stage 1 is buildup of elastic strain. Stage 2 is development of cracks. Stage 3 is influx of ground water.

The observed v-shaped pattern prior to the three main shocks clearly progresses in a sequence of three stages (Kuo et al. 2006). The sequence of events for radon anomalies prior to the 2003 M_w = 6.8 Chengkung, 2006 M_w = 6.1 Taitung, and 2008 M_w = 5.4 Antung earthquakes were characterized into three stages in Figs. 11a, 11b, and 11c, respectively (Kuo et al. 2006, 2010a). During Stage 1, the radon concentration in ground water was fairly stable; there was an accumulation of tectonic strain and a slow, steady increase of regional stress. The Antung hot spring is a fractured aquifer with limited recharge surrounded by ductile mudstone (Chen & Wang 1996). When the regional stress increased under these geological conditions, dilation of brittle rock masses occurred at a rate faster than the rate at which ground water could recharge into the newly created rock cracks (Brace et al. 1966; Nur 1972; Scholz et al. 1973). During this stage (Stage 2 in Fig. 11), gas saturation and two phases (vapor and liquid) developed in the rock cracks. The radon in ground water volatilized into the gas phase and the radon concentration in ground water decreased. Stage 3 started at the point of minimum radon concentration when the water saturation in cracks and pores began to increase again. During this stage (Stage 3 in Fig. 11), the radon concentration in groundwater increased and recovered to the previous background level before the main shock.

Figs. 11a, 11b, and 11c show that during Stage 2 prior to the 2003 M_w = 6.8 Chengkung, 2006 M_w = 6.1 Taitung, and 2008 M_w = 5.4 Antung earthquakes the radon concentration in ground water kept decreasing for a significantly long period of 45, 47, 31 days, respectively. Combining the use of box-and-whisker plot, the v-shaped radon pattern shown in Figs. 10 and 11 prior to the 2003 M_w = 6.8 Chengkung, 2006 M_w = 6.1 Taitung, and 2008 M_w = 5.4 Antung earthquakes can be clearly distinguished from other scattering radon data which appear to be related to smaller local earthquakes and aftershocks.

As shown in Fig. 11, radon decreased from background levels of 787 ± 42, 762 ± 57, and 700 ± 57 pCi/L to minima of 326 ± 9, 371 ± 9, and 480 ± 43 pCi/L prior to the 2003 M_w = 6.8 Chengkung, 2006 M_w = 6.1 Taitung, and 2008 M_w = 5.4 Antung earthquakes, respectively. Kuo et al. (2010b) recognized that the observed precursory minimum in radon concentration decreases as the local earthquake magnitude increases. Kuo et al. (2010b) also proposed an empirical correlation for local applications as follows.

$$C_w = 1063 - 110M_w \tag{2}$$

where C_w is the radon minimum in groundwater observed in well D1 during an anomalous decline, pCi/L; M_w is the earthquake magnitude. Eq. (2) did not take the initial stable radon concentration in groundwater precursory to each radon anomaly into account. Our observations in well D1 indicate that the initial stable radon concentration in groundwater precursory to each radon anomaly does vary occasionally. Eq. (2) will be improved by taking into account the initial stable radon concentration in groundwater precursory to each radon anomaly.

Based on radon phase behavior and rock dilatancy, Kuo et al. (2006, 2010a) developed a mechanistic model correlating the observed decline in radon with the volumetric strain change. The model consists of two parts, i.e., the radon-volatilization model and the rock-dilatancy model. The radon-volatilization model can be expressed as follows.

$$C_0 = C_w (H \times S_g + 1) \quad (1)$$

where C_0 is initial radon concentration in groundwater precursory to each radon anomaly, pCi/L; C_w is the radon minimum in groundwater observed in well D1 during an anomalous decline, pCi/L; S_g is gas saturation, fraction; H is Henry's coefficient for radon at formation temperature (60 ℃), dimensionless. The radon-volatilization model correlates the radon decline to the gas saturation for a given fracture porosity.

The rock-dilatancy model can be expressed as follows.

$$d\varepsilon \cong \phi S_g \quad (3)$$

where $d\varepsilon$ is volumetric strain, fraction; ϕ is initial fracture porosity before rock dilatancy, fraction; S_g is gas saturation, fraction. The rock-dilatancy model correlates the volumetric strain to the gas saturation for a given fracture porosity.

Combining the radon volatilization and rock dilatancy models, equations (1) and (3), the groundwater radon concentrations can be correlated to the strain changes associated with earthquake occurrences as follows.

$$d\varepsilon \cong \frac{\phi}{H} \left(\frac{C_0}{C_w} - 1 \right) \quad (4)$$

where $\left(\frac{C_0}{C_w} - 1 \right)$ is normalized radon decline, dimensionless. The Henry's coefficients (H) at formation temperature (60 ℃) is 7.91 for radon (Clever, 1979). Given an average fracture porosity of 0.00003 for the Antung hot spring, Eq. (4) can be used to calculate the crust strain.

Using the radon minima precursory to the 2003, 2006, and 2008 quakes, the calculated crust –strain and observed dimensionless radon-decline are plotted as a function of earthquake magnitude in Fig. 12. The best-fitting straight line is obtained by means of the least-square method with a high value of the sample correlation squared regression coefficient (i.e., R^2 = 0.9802). The regressed equations are as follows.

$$d\varepsilon = 2.5893 M_w - 12.0948 \quad (5)$$

$$\left(\frac{C_0}{C_w} - 1 \right) = 0.6827 M_w - 3.189 \quad (6)$$

where C_0 is initial radon concentration in groundwater precursory to each radon anomaly, pCi/L; C_w is the radon minimum in groundwater observed in well D1 during an anomalous decline, pCi/L; M_w is the earthquake magnitude; $d\varepsilon$ is volumetric strain, fraction. Eq. (6) would be quite useful locally in predicting earthquake magnitude nearby the Chihshang fault from the radon minimum observed in well D1 during an anomalous decline.

Three precursory radon minima associated with nearby large and moderate earthquakes have been recorded from the same monitoring well (D1). The same v-shaped pattern

recognized in all the three recurrent radon anomalies and the threshold concentration are useful for the early warning of potentially disastrous earthquakes ($M_w > 6.0$) in the southern segment of coastal range and longitudinal valley of eastern Taiwan.

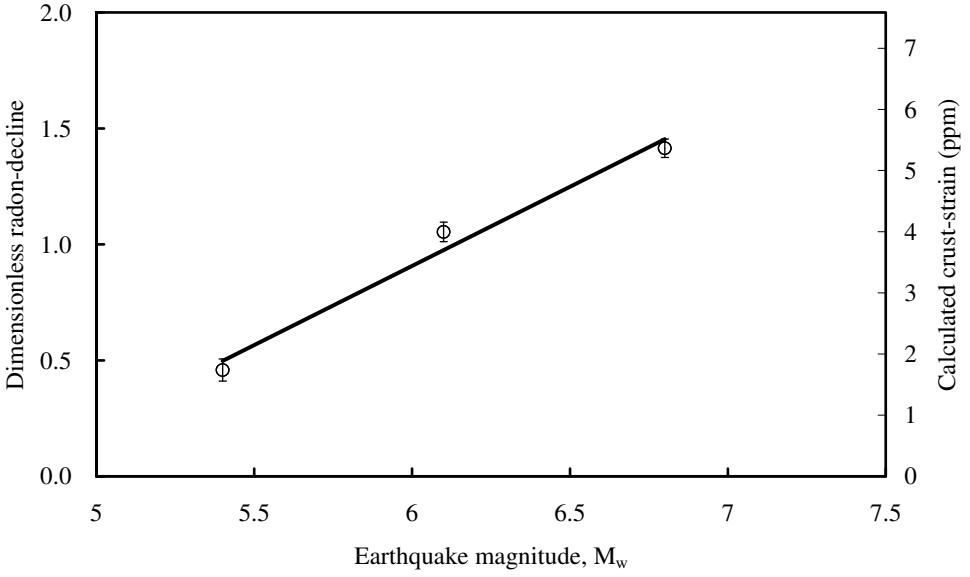

Fig. 12. Calculated crust-strain ($d\varepsilon$) and observed radon-decline ($\frac{C_0}{C_w} - 1$) at well D1 that occurred on December 10, 2003, April 1, 2006, February 17, 2008 as a function of earthquake magnitude (M_w). Radon-concentration errors are ±1 standard deviation.

6. Conclusions

Since July 2003, we have recorded three recurring radon anomalies (precursory to the 2003 M_w = 6.8 Chengkung, 2006 M_w = 6.1 Taitung, and 2008 M_w = 5.4 Antung earthquakes) at well D1, located at the Antung hot spring. The local geological conditions near the Antung hot spring with well D1 situated in a fractured aquifer surrounded by ductile mudstone and the in-situ volatilization of groundwater radon were attributed for causing the recurrent radon anomalies precursory to the nearby large and moderate earthquakes. The following conclusions can be drawn from this study.

1. Radon anomalous declines in groundwater consistently recorded prior to local large and moderate earthquakes near the Antung hot spring in eastern Taiwan provide the reproducible evidence to catch radon precursors under suitable geological conditions.
2. "A low-porosity fractured aquifer surrounded by ductile formation in a seismotectonic environment" is a suitable geological site to consistently catch precursory declines in groundwater radon and dissolved gases prior to local large and moderate earthquakes.
3. Radon partitioning into the gas phase (the mechanism of in-situ radon volatilization) may explain the radon anomalous declines in groundwater consistently recorded prior to local large and moderate earthquakes near the Antung hot spring in eastern Taiwan
4. The observed precursory minimum in radon concentration decreases as the earthquake magnitude increases. The observed relationship between radon minima and earthquake magnitude provides a possible means to forecast local disastrous earthquakes.

7. Acknowledgments

Supports by the National Science Council (NSC-96-2116-M-006-012, NSC-96-2738-M-006-004, NSC-97-2745-M-006-001, NSC-98-2116-M-006-016, and NSC-99-2116-M-006-019) and Central Geological Surveys (98-5226904000-05-02 and 99-5226904000-05-02), Radiation Monitoring Center, and Institute Earth Sciences of Academia Sinica of Taiwan are appreciated.

8. References

Angelier, J.; Chu, H. T.; Lee, J. C. & Hu, J. C. (2000). Active faulting and earthquake hazard: The case study of the Chihshang fault, Taiwan. *Journal of Geodynamics*, Vol. 29, pp. 151-185, ISSN 0264-3707

Brace, W. F.; Paulding, B. W. Jr. & Scholz, C. (1966). Dilatancy in the fracture of crystalline rocks. *Journal of Geophysical Research*, Vol. 71, pp. 3939-3953, ISSN 2156–2202

Chen, W. S. & Wang, Y. (1996). Geology of the Coastal Range, eastern Taiwan, In: *Geological Series of Taiwan 7*, F. C. Chien, Central Geological Survey, ISBN 957-00-6978-3, Taiwan

Clever, H. L. (1979). Krypton, Xenon and Radon-Gas Solubilities, In: *Solubility Data Series 2*, H. L. Clever & R. Battino, Pergamon Press, ISBN 0-08-022352-4, Oxford, UK

Hauksson, E. (1981). Radon content of groundwater as an earthquake precursor: Evaluation of worldwide data and physical basis. *Journal of Geophysical Research*, Vol. 86, pp. 9397-9410, ISSN 2156–2202

Hsu, T. L. (1962). Recent faulting in the Longitudinal Valley of eastern Taiwan. *Memoir of the Geological Society of China*, Vol. 1, pp. 95-102, ISSN 0578-1825

Igarashi, G.; Saeki, S.; Takahata, N.; Sumikawa, K.; Tasaka, S.; Sasaki, Y.; Takahashi, M. & Sano, Y. (1995). Ground-water radon anomaly before the Kobe earthquake in Japan. *Science*, Vol. 269, pp. 60-61, ISSN 1095-9203

Kuo, M. C. Tom; Fan, K.; Kuochen, H. & Chen, W. (2006). A mechanism for anomalous decline in radon precursory to an earthquake. *Ground Water*, Vol. 44, pp. 642-647, ISSN 1745-6584

Kuo, T.; Lin, C.; Chang, G.; Fan, K.; Cheng, W. & Lewis, C. (2010a). Estimation of aseimic crustal-strain using radon precursors of the 2003 M 6.8, 2006 M 6.1, and 2008 M 5.0 earthquakes in eastern Taiwan. *Natural Hazards*, Vol. 53, pp. 219-228, ISSN 1573-0840

Kuo, T.; Su, C.; Chang, C.; Lin, C.; Cheng, W.; Liang, H.; Lewis, C. & Chiang, C. (2010b). Application of recurrent radon precursors for forecasting large earthquakes (M_W > 6.0) near Antung, Taiwan. *Radiation Measurements*, Vol. 45, pp. 1049-1054, ISSN 1350-4487

Liu, K. K.; Yui, T. F.; Yeh, Y. H.; Tsai, Y. B. & Teng, T. L. (1985). Variations of radon content in groundwaters and possible correlation with seismic activities in northern Taiwan. *Pure and Applied Geophysics*, Vol. 122, pp. 231-244, ISSN 1420-9136

Lee, J. C.; Angelier, J.; Chu, H. T.; Hu, J. C.; Jeng, F. S. & Rau, R. J. (2003). Active fault creep variations at Chihshang, Taiwan, revealed by creep meter monitoring, 1998-2001. *Journal of Geophysical Research*, Vol. 108, pp. 2528-2548, ISSN 2156–2202

Lowry, D. (1991). Measuring low radon levels in drinking water supplies. *Journal American Water Works Association*, Vol. 83, pp. 149-153, ISSN 1551-8833

Noguchi, M. (1964). Radioactivity measurement of radon by means of liquid scintillation fluid. *Radioisotope*, Vol. 13, pp. 362-366, ISSN 0033-8303

Noguchi, M. & Wakita, H. (1977). A method for continuous measurement of radon in groundwater for earthquake prediction. *Journal of Geophysical Research*, Vol. 82, pp. 1353-1357, ISSN 2156–2202

Nur, A. (1972). Dilatancy, pore fluids, and premonitory variations of ts/tp traval times. *Bulletin of the Seismological Society of America*, Vol. 62, pp. 1217-1222, ISSN 1943-3573

Prichard, H. M. & Gesell, T. F. (1977). Rapid measurements of 222Rn concentrations in water with a commercial liquid scintillation counter. *Health Physics*, Vol. 33, pp. 577-581, ISSN 1538-5159

Prichard, H. M.; Venso, E. A. & Dodson, C. L. (1992). Liquid-Scintillation analysis of 222Rn in water by alpha-beta discrimination. *Radioactivity and Radiochemistry*, Vol. 3, pp. 28-36, ISSN 1045-845X

Scholz, C. H.; Sykes, L. R. & Aggarwal, Y. P. (1973). Earthquake prediction: A physical basis. *Science*, Vol. 181, pp. 803-810, ISSN 1095-9203

Teng, T.L. (1980). Some recent studies on groundwater radon content as an earthquake precursor. *Journal of Geophysical Research*, Vol. 85, pp. 3089-3099, ISSN 2156–2202

Toutain, J. P. & Baubron J. C. (1999). Gas geochemistry and seismotectonics: a review. *Tectonophysics*, Vol. 304, pp. 1–27, ISSN 0040-1951

Wakita, H.; Nakamura, Y.; Notsu, K.; Noguchi, M. & Asada, T. (1980). Radon anomaly: A possible precursor of the 1978 Izu-Oshima-kinkai earthquake. *Science*, Vol. 207, pp. 882-883, ISSN 1095-9203

Yu, S. B. & Kuo, L. C. (2001). Present-day crustal motion along the Longitudinal Valley Fault, eastern Taiwan. *Tectonophysics*, Vol. 333, pp. 199-217, ISSN 0040-1951

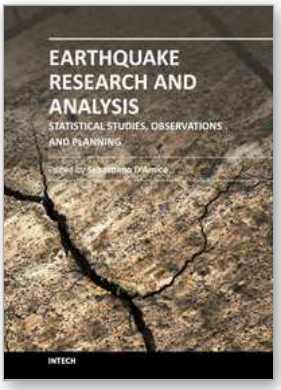

Earthquake Research and Analysis - Statistical Studies, Observations and Planning

Edited by Dr Sebastiano D'Amico

ISBN 978-953-51-0134-5
Hard cover, 460 pages
Publisher InTech
Published online 02, March, 2012
Published in print edition March, 2012

The study of earthquakes plays a key role in order to minimize human and material losses when they inevitably occur. Chapters in this book will be devoted to various aspects of earthquake research and analysis. The different sections present in the book span from statistical seismology studies, the latest techniques and advances on earthquake precursors and forecasting, as well as, new methods for early detection, data acquisition and interpretation. The topics are tackled from theoretical advances to practical applications.

InTech Europe
University Campus STeP Ri
Slavka Krautzeka 83/A
51000 Rijeka, Croatia
Phone: +385 (51) 770 447
Fax: +385 (51) 686 166
www.intechopen.com

InTech China
Unit 405, Office Block, Hotel Equatorial Shanghai
No.65, Yan An Road (West), Shanghai, 200040, China
中国上海市延安西路65号上海国际贵都大饭店办公楼405单元
Phone: +86-21-62489820
Fax: +86-21-62489821